Urbanization and its impact on Land Surface Temperature: A case study in Coastal Odisha

Abstract

The East and Southeastern Coastal Plain Zone (ESECPZ) of Odisha, situated along the eastern coast of India, present a mosaic of urban and rural regions. The present study aimed to estimate the land use land cover change and extent of urbanization in ESECPZ over the span of two decades, from 2000 to 2020. Multi-year Landsat data were undergone supervised maximum likelihood classification for estimating the LULC change. The ESECPZ of Odisha underwent substantial transformations during the study period. Forest cover decreased from 33.95% to 18.98%, agricultural land decreased from 24.98% to 21.84%, as against the settlements, which surged from 21.52% to 39.67%. The maximum, minimum and average Land Surface Temperature (LST) showed steady increase during the period of study. About 5°C increase in the minimum LST range and 3°C increase in maximum LST were recorded. The increase in LST was attributed to the expansion of settlement areas and reduction in the vegetation cover due to population growth and urbanization. Normalized Difference Vegetation Index (NDVI) and Normalized Difference Built-up Index (NDBI) showed gradual decreasing and increasing trends, respectively. Strong positive correlation was found between LST and NDBI while a strong negative correlation was found between LST and NDVI during all the years under study. This research has provided valuable insights into the often-overlooked impacts of urbanization LST, vegetation covers etc. These findings offer a positive perspective for the future and can inform and bolster forward-thinking initiatives and applications aimed at addressing these challenges.

Keywords – Landsat, LST, NDBI, NDVI, Urbanization

1. Introduction

Rapid urbanization and industrialization are two interconnected phenomena that are posing significant challenges to the planet Earth (Bai *et al*., 2017). The rapid influx of people into urban areas, driven by factors such as migration and birth rates, cause urban areas to grow at an alarming rate (Virtudes *et al*., 2017). As a result, population growth, coupled with the increasing

industrialization and production demands, poses immense pressure on the Earth's resources and ecosystems (Motesharrei *et al*., 2016), leading to environmental degradation, climate change, and resource scarcity. It has been noted that the amount of land covered by urbanized areas will increase twice over the course of the next 40 years and most people on the planet would be impacted by anthropogenic climate change in urban contexts (Zhao *et al*., 2019). Therefore, the importance of local urban governments in addressing climate change is highly emphasized (Khosla and Bhardwaj, 2019; Parapurath et al., 2025a).

The degree of temperature variation between urban and rural areas tends to increase with higher levels of urbanization (Tam *et al*., 2015; Chapman *et al*., 2017; Chen *et al*., 2017; Peng *et al*., 2021). Notably, natural cooling effects are eliminated when natural land cover is replaced with infrastructure, concrete, and industrial activity (Mohajerani *et al*., 2017). Moreover, one of the harmful effects of urbanization on Land Surface Temperature (LST) is the creation of heat islands (Tam *et al*., 2015). Heat islands are localized areas within urban environments that experience significantly higher temperatures compared to the surrounding rural areas (Mardiatmoko & Hatulesila, 2020). These heat islands are caused by the high concentration of buildings, roads, and concrete surfaces in urban areas, which absorb and retain more heat from the sun compared to natural landscapes (Irfeey et al., 2023). The high LST can make urban areas extremely uncomfortable and even dangerous to live in, especially during heatwaves (Macintyre *et al*., 2018; Wei *et al*., 2024). Additionally, the elevated LST contribute to increased energy consumption for cooling purposes, leading to higher greenhouse gas emissions (Van Vuuren *et al*., 2017). As urban areas become more developed, they contribute to an increase in the air temperature through the release of heat from buildings, vehicles and industrial activities (Santos *et al*., 2020). According to Argüeso *et al*. (2014), it is routinely predicted that the minimum temperature will rise faster in recently developed areas, while the changes are apparent throughout the year. Furthermore, as the global climate changes, cities are increasingly vulnerable to extreme weather events such as heatwaves, storms, and flooding (Chen *et al*., 2014; Wang *et al*., 2015). The faster rate of change in climate variables combined with the occurrences of extreme weather events (Senapati et al., 2024; Parapurath et al., 2025b; Subba Rao et al., 2025) have significant impact.

Throughout the twentieth century, the expansion of urbanization globally has led to a decline in tree cover within urban areas, largely driven by the demand for land development (Güneralp *et al*., 2020). The transformation of agricultural lands into urban areas has also

disrupted the local hydrological cycle, leading to reduced groundwater recharge and increased surface runoff (Nayak and Nandimandalam, 2023). However, satellite-based remote sensing has been proved to be a valuable tool for assessing and monitoring urbanization in India (Radočaj *et al*., 2020). It allows decision makers to precisely monitor the changes in land cover and provides crucial information for public policy planning and the management of earth resources, enabling decision makers to address issues like changes of land surface temperature, soil moisture, surface water resources, extent of agriculture etc. (Swain *et al*., 2017; Nanda *et al*., 2023; Ghosh *et al.,* 2024). In order to monitor the extent of urbanization over time, researchers successfully harnessed the potential of high-resolution satellite datasets viz., Landsat, MODIS (Moderate Resolution Imaging Spectroradiometer), and Sentinel (Sidiqui *et al*., 2016; Bonafoni and Keeratikasikorn, 2018). While numerous studies have gauged the warmth of urban areas by measuring air temperature through ground-based observation stations, ~~but~~ monitoring LST provides a more comprehensive perspective on the thermal dynamics of these regions because among the indicators, LST is a valuable indicator that offers crucial insights into the physical characteristics of the Earth's surface and its influence on climate, which in turn affects various environmental processes (Wu *et al*., 2019). Additionally, several researchers computed different satellite- derived indices such as Enhanced Vegetation Index (EVI), Normalized Difference Built-up Index (NDBI), Normalized Difference Vegetation Index (NDVI) etc., to estimate the extent of urbanization, and vegetation cover (Karanam and Neela, 2017; Kumari *et al*., 2018; Bouhennache *et al*., 2019; Parapurath et al., 2020). So, incorporating Remote Sensing (RS) and Geographic Information System (GIS) enables comprehensive mapping by integrating diverse geospatial data for enhanced analysis (Prakash et al., 2025).

In the coming decades, India will experience the greatest urban shift on record world-wide because there are currently more than 50 urban agglomerations in the nation with a million citizens. Further, it is anticipated that India's urban population would double to over 800 million people (Chakrabarti, 2001). The increasing urbanization in India has led to significant changes in land-use patterns. These changes coupled with climate change impacts had created a complex and challenging situation for the country (Roy et al., 2022). Being no exception, Odisha, the state on the east coast of India, is experiencing urbanization ~~occurring~~ at a steady pace (Zhao *et al*., 2017; Lohani, 2022). As a result of urbanization, there have been significant changes in the climate of Odisha, including extreme high temperature, heat waves, altered precipitation patterns, and the formation of urban heat islands (Gogoi *et al*., 2019).

Therefore, the present study aims to monitor the spatial and temporal changes in land use & land cover patterns for understanding the urbanization extent of East and Southeastern Coastal Plain Zone of Odisha over 2000-2020 and to assess the impact of urbanization on land surface temperature using geospatial technology.

2. Materials and methods

2.1 Study area

The East and Southeastern Coastal Plain Zone (ESECPZ) of Odisha (Fig. 1) is geographically distributed along the 290 km long seacoast and stretched to 100–120 km inland from the sea (Behera et al., 2023). The present study was conducted in the five districts of ESECP viz. Puri, Kendrapara, Jagatsinghpur, Khordha, and Nayagarh; ~~among which three districts namely~~ Puri, Kendrapara and Jagatsinghpur are located along the coast of the Bay of Bengal. The demographic profile of the districts has been given in table 1. The zone is characterized by a hot, humid tropical climate with predominantly lateritic, alluvial and saline soils. The study area receives an average annual rainfall of 1450 mm, about 80% of which falls during the monsoon season. The average summertime temperature is 39°C, while the average winter-low temperature is 11.5°C (Sahu *et al*., 2021; Dugal *et al*., 2022).

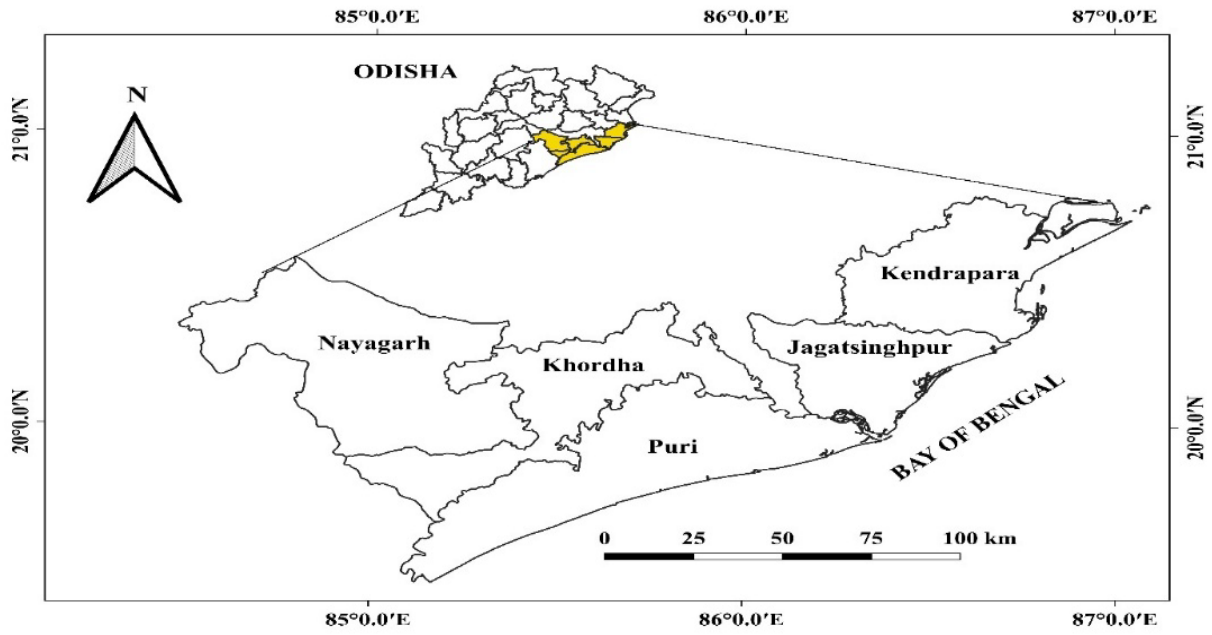

Fig. 1 Geographical location of the East and South Eastern Coastal Plain Zone (ESECPZ) of Odisha

Table 1 Demographic profile of the ESECPZ of Odisha

District	Geographic area (km^2)	Population density per sq. km		
		1991	2001	2011
Puri	3,479	375.2	431.9	488.3
Kendrapara	2,644	434.8	492.4	544.8
Jagatsinghapur	1,668	560.0	634.2	681.6
Khordha	2,813	534.0	667.4	800.5
Nayagarh	3,890	201.2	222.2	247.5

2.2 Data

Multi-year Landsat data were used in the present study for land use and land-cover monitoring. In order to monitor the decadal changes in LULC and thereby urban extent, Landsat 7 ETM+, Landsat 5 MSS and Landsat 8 OLI and TRIS data were collected for the year 2000, 2010 and 2020 respectively, from open data archive of United State Geological Survey (USGS) via www.earthexplorer.usgs.gov. Imageries taken in the visible, near infra-red and shortwave infra-red channels were used for land-use classification while the imageries taken in the thermal infra-red channel were used for estimating Land Surface Temperature. The study area was covered by two Landsat tiles (139/46 and 140/46). So, two data were downloaded for each year. The details of the data used in the study have been given in the table 2. Google Earth Pro imageries were used for generating the Ground truth points for training the classification and testing the accuracy.

Table 2 Details of the data used in the study

Year	Acquisition Date	Path/ Row	Satellite and Sensors	Bands used	Resolution
2000	17/12/2000 10/12/2000	139/46 140/46	Landsat 7 ETM+ (Enhanced Thematic Mapper)	Band 1: Blue (0.45-0.52 µm)	30 m
				Band 2: Green (0.52-0.60 µm)	30 m
				Band 3: Red (0.63-0.69 µm)	30 m
				Band 4: Near-Infrared (0.76-0.90 µm)	30 m
				Band 5: Near-Infrared (1.55-1.75 µm)	30 m
2010	25/04/2010 18/04/2010	139/46 140/46	Landsat 5 MSS (Multispectral Scanner)	Band 6: Thermal (10.40-12.50 µm)	120 m (MSS) 60 m (ETM+)
				Band 7: Mid-Infrared (2.08-2.35 µm)	

2020	28/03/2020 03/03/2020	139/46 140/46	Landsat 8 OLI (Operational Land Imager) and TIRS (Thermal Infrared Sensor)	Band 2: Visible (0.450-0.51 µm)	30 m
				Band 3: Visible (0.53-0.59 µm)	30 m
				Band 4: Red (0.64-0.67 µm)	30 m
				Band 5: Near-Infrared (0.85-0.88 µm)	30 m
				Band 6: SWIR 1 (1.57-1.65 µm)	30 m
				Band 7: SWIR 2 (2.11-2.29 µm)	30 m
				TIRS Band 10: TIRS 1 (10.6-11.19 µm)	100m
				Band 11: TIRS 2 (11.5-12.51 µm)	100 m

2.3 Image processing and classification

The level-1 satellite data was pre-processed for radiometric calibration and atmospheric correction in Quantum GIS (QGIS) 3.16.8 software. Semi-automatic Classification Plugin (SCP) was applied in radiometric calibration. DOS 1 (Dark Object Subtraction) algorithm was used for atmospheric correction in the present study. Prominently, two tiles viz. 139/ 46 and 140/46 were mosaicked for each image date. The subset image is undergone supervised maximum likelihood classification using the training dataset obtained from Google Earth Pro. The sample points of the training as well as testing datasets were taken in a stratified way and validated using different bands combination (Khan and Das, 2022) as given in ~~the~~ Table 3. The study area was classified into five LULC classes, namely Agriculture, Barren land and Rocks, Forest, Settlements and Water bodies (Table 4), using ArcGIS 10.8 software.

Table 3 Landsat band combination applied in the present study

Features	Band combination for Landsat 5 and 7	Band combination for Landsat 8
Agriculture	7, 4, 2	6, 5, 2
Forest	4, 5, 3	5, 4, 3
Barren land and Rocks	3, 2, 1	5, 6, 4
Settlements	4, 3, 2	7, 6, 4
Water bodies	3, 2, 1	5, 6, 4

Table 4 Description of different LULC classes

Class	Features	Description
1	Agriculture	Cropping lands with crops
2	Barren land and Rocks	Unused lands and uncultivated lands
3	Forest	Dense and less dense vegetation
4	Settlements	Residential and Concrete structures
5	Water bodies	Ponds, Lakes, Canals and River

2.4 Accuracy assessment

In order to validate the classification results, the testing dataset prepared using Google Earth Pro images was used. However, classification accuracies were measured in terms of user's accuracy, producer's accuracy and overall accuracy. The kappa coefficient, an indicator of how well the classified map resulted from the maximum likelihood classification and the source data are agreed or accurate was calculated following the formula of Stehman (1996). Kappa coefficient is less influenced by variations in sample sizes among different classes, making it a more dependable and robust indicator of classification accuracy and the value of the kappa coefficient ranges from 0.1 to 1.0.

$$K = \frac{N \sum_{i=1}^{k} nij - \sum_{i=1}^{k} ni + nj}{N^2 - \sum_{i-1}^{k} ni - nj}$$

where,

K = number of rows in error matrix; n_{ij} = number of observations in row i and column j; n_i = total number of observations in row i; n_j = total number of observations in column j; N = total number of observations in matrix

Kappa coefficient values can be categorized into five groups (Meer and Mishra, 2020), as given in the following table 5.

Table 5 Categories of Kappa coefficient values

Kappa coefficient values	Categories
0-0.20	Slight agreement
0.21- 0.40	Fair agreement
0.41- 0.60	Moderate agreement
0.61- 0.80	Substantial agreement
0.81- 1.00	Almost perfect agreement

2.5 Estimation of Land Surface Temperature (LST)

The Land Surface Temperature (LST) is calculated using Landsat thermal bands using the following equations adopted by Hakan (2016).

$$\mathrm{LST} = \frac{\mathrm{T_b}}{[1 + \left(\lambda * \frac{\mathrm{T_b}}{\mathrm{C_2}}\right) * \ln(\varepsilon)]}$$

where, T_b is at-Satellite Brightness Temperature, λ is wavelength of emitted radiance, C_2 = 1.4388 X 10^{-2} mK and ε is emissivity (typically 0.95)

$$T_b = \frac{K_2}{(\ln(K_1 * \frac{\varepsilon}{L} + 1))}$$

where, K_1 is the sensor dependent calibration constant 1 and K_2 is the sensor dependent calibration constant 2. ε is emissivity (typically 0.95), and L is the spectral radiance. C_2 is calculated using the following formula

$$C_2 = h * \frac{c}{s}$$

where, h is Planck's constant = 6.626 × 10^{-34} Js; c is the velocity of light = 2.998 × 10^8 m/s, and s is the Boltzmann constant = 1.38 × 10^{-23} J/K.

2.6 Computation of NDVI and NDBI

In order to determine the vegetation condition and urbanization condition, two indices viz. Normalized Difference Vegetation Index (NDVI) and Normalized Difference Built-up Index (NDBI) computed using the formulae adopted by Alademomi *et al*. (2022).

$$NDVI = \frac{R_{NIR} - R_R}{R_{NIR} + R_R}$$

$$NDBI = \frac{R_{SWIR} - R_{NIR}}{R_{SWIR} + R_{NIR}}$$

Where, R_{NIR} = Reflectance in near infra-red band; R_R= Reflectance in red band and R_{SWIR}= Reflectance in shortwave infra-red band.

2.7 Assessing the relationship of urbanization with LST and air temperature

To determine the impact of urbanization on LST, correlation analysis was carried out between LST and estimated the area under Settlements class. The influence of surface vegetation cover and built-up area on the surface temperature was examined by the correlation of LST with NDVI and NDBI. The image correlation over the years 2000, 2010, and 2020 was carried out in ArcGIS 10.8 to formally demonstrate the link between LST and vegetation indices.

3 Results

3.1 Decadal LULC change with special reference to urban extent

The maximum likelihood classification of multi-year Landsat data yielded in decadal LULC changes of the ESECPZ of Odisha. The thematic LULC maps for the years 2000, 2010 and 2020 have been represented by the figure 2a, 2b and 2c respectively.

The maximum likelihood classification for the year 2000 recorded an overall accuracy of 89.66 % with the kappa coefficient value of 0.87 (Table 6), demonstrating the reliability and acceptability of LULC classification. The results revealed that in the year 2000, forest land exhibited the largest coverage. The estimated area under different LULC classes during the entire study period have been given in ~~the~~ Table 7. It was estimated that forest covered 4952.21 sq. km area occupying about 34 % of the total geographical area of in 2000. Agricultural land exhibiting the second largest coverage occupied 3644.36 sq. km area, which was about 25%. Settlements came third with 3138.67 sq. km area, followed by the Barren and rock lands, covering 3138.67 sq. km and 1803.44 sq. km respectively. Waterbodies had the smallest coverage, with 1047.92 sq. km area, which occupied only 7.2% of the total area.

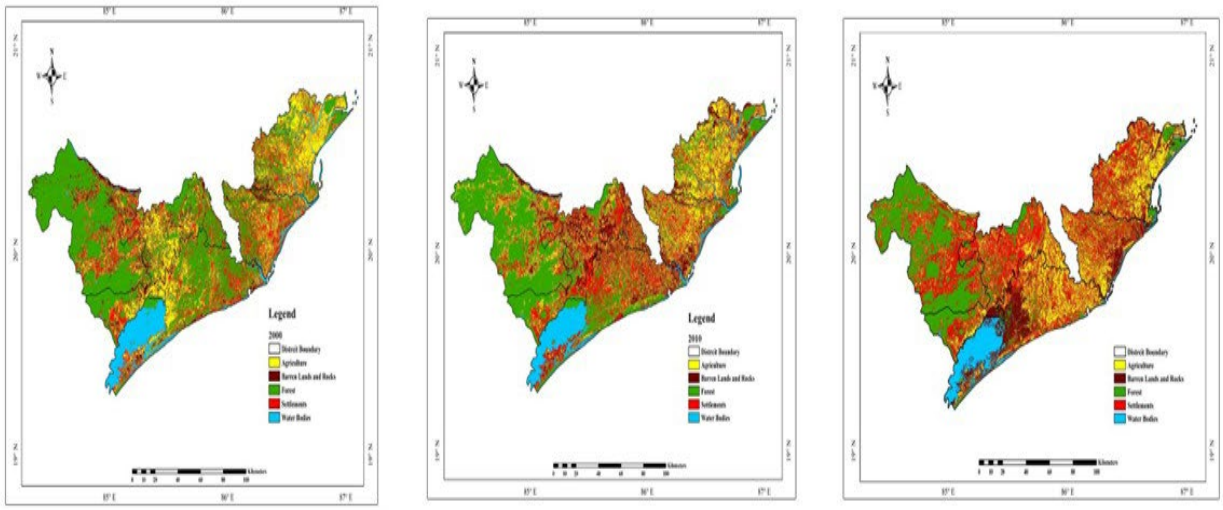

a. 2000 **b. 2010** **c. 2020**

Fig. 2(a-c) LULC maps of the ESECPZ of Odisha over 2000-2020

Table 6 Accuracies of LULC classification

Years	Overall Accuracy (%)	Kappa coefficient
2000	89.66 %	0.87
2010	88.33 %	0.85

2020	90.67 %	0.88

Over 2000-2010, the study area experienced a notable decrease in the area under forest. It was estimated that forest area was reduced by about 32.8% during this time period (Table 7). About 23% (3326.25 sq. km) of ESECPZ was classified as forest land in 2010. Agricultural land also followed the declining trend with a reduction of about 3.5% of that in 2000. In the year 2010, Agricultural land covered almost 24% of the total area. On the contrary, the Settlements areas increased in 2010 and estimated as 4712.00 sq. km occupying about 32 %. However, less changes were observed in the area under the Barren and rock lands and waterbodies covering about 14 % (1976.05 sq. km) and 7.2 % (1055.05 sq. km) respectively. Overall, the LULC classification for 2010 also resulted in high accuracy, as indicated by the overall accuracy of 88.33 % and a kappa coefficient value of 0.85.

Table 7 Changes in LULC classes (sq.km) of East and South Eastern Coastal Plain Zone of Odisha from 2000 to 2020

Land use classes	2000	2010		2020			
	Area (sq.km)	Area (sq.km)	Change over 2000 (sq.km)	Area (sq.km)	Change over 2010 (sq.km)	Change over 2000 (sq.km)	% change over 2000
Agriculture	3644.36	3517.25	-127.11	3185.53	-331.72	-458.83	12.59
Barren Land	1803.44	1976.05	172.61	1779.93	-196.12	-23.51	1.30
Forest	4952.21	3326.25	-1625.96	2767.94	-558.31	-2184.27	44.10
Settlements	3138.67	4712.00	1573.33	5787.2	1075.20	2648.53	84.38
Water Bodies	1047.92	1055.05	7.13	1066	10.95	18.08	1.72

The LULC classification for the year 2020 revealed further decrease in the areas under forest and agricultural land by 44% and 12.5% respectively, as compared to that in 2000, and 16.78% and 9%, as compared to that in 2010. It was found that forest occupied about 19 % (2767.94 sq. km) while agricultural land covered about 22% (3185.53 sq. km). The area under the Barren land, with 1779.93 sq. km area, experienced a slight decrease of 196.12 sq. km when compared to the year 2010. Conversely, there was a substantial increase in the settlement area, with 5787.20 sq. km area, covering almost 40 % of the total geographical area of the study zone.

Notably, there was a marginal increase in the area, covered by waterbodies, occupying 1066.00 sq. km area. The overall accuracy of the LULC classification was calculated as 90.67% with the kappa coefficient value of 0.88.

The results inferred that the supervised classification demonstrated almost 80 % accurate classification for the settlements. The highest user's accuracy of 87.3% was obtained in the year 2020, followed by 80.7% and 78.2 % for the year 2000 and 2010 respectively. On the other hand, the maximum producer's accuracy was recorded in the year 2000 and calculated as 93.8%. Producer's accuracies for the year 2010 and 2020 were calculated as 78.2% and 81.4% respectively. During the study period, a steady rise in the area under settlements was noticed. In the year 2010, the Settlements area increased by almost 50% of that in 2000, which implies ~~that~~ an addition of 1573.33 sq. km under the settlement class in 2010. Similarly, in the next decade (over 2010-2020), the area under Settlements increased by about 23%. Overall, the settlement area observed a highly significant growth of about 84% from 2000-2020.

3.2 Spatiotemporal variation of LST

Landsat thermal bands were used to estimate the Land Surface Temperature (LST) of the study year during 2000, 2010 and 2020 and the results so obtained ~~have been~~ represented in ~~the~~ figure 3a, 3b and 3c, respectively. In 2000, LST varied from 18.43°C to 42.96°C with an average LST of 30.14°C (Table 8), although, the average, maximum and minimum LST were found to increase steadily in 2010 and 2020. The average LST increased by 1.68 °C from 2000 to 2010 and 2.97 °C from 2010 to 2020. On the other hand, the maximum and minimum LST increased by 0.8 °C and 2.43°C respectively, from 2000 to 2010. Further increase in the maximum and minimum LST by 2.09 °C and 2.85°C was recorded from 2010 to 2020. Considering the entire study period, the average LST was found to rise by 4.65 °C, while the maximum and minimum LST increased by 2.92°C and 5.28°C, respectively.

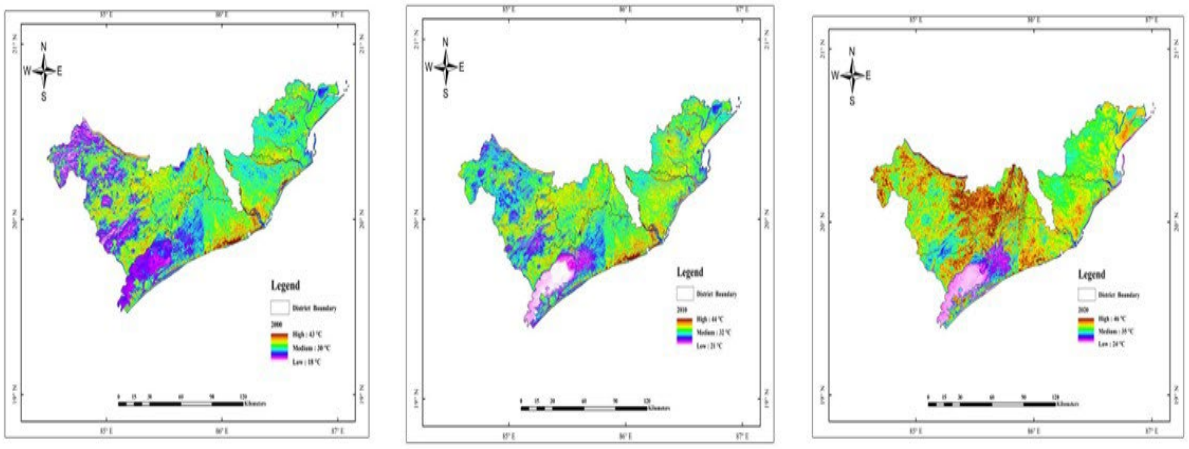

a. 2000 **b. 2010** **c. 2020**

Fig. 3(a-c) Spatial variations in the LST of the ESECPZ of Odisha over 2000-2020

Table 8 Temporal changes of LST ranges and its relationship with settlements

LST	2000	2010	2020	Percentage increase over 2000 (%)	Correlation coefficient between LST and Settlements
Maximum LST(°C)	42.96	43.79	45.88	6.79	0.950
Minimum LST (°C)	18.43	20.86	23.71	28.64	0.806
Average LST (°C)	30.14	31.82	34.79	15.42	0.955

3.3 Spatiotemporal Variation of NDVI and NDBI

In order to estimate the spatial variation of vegetation cover over the two decades, NDVI was computed for the three years (2000, 2010 and 2020) and the thematic NDVI maps were represented in ~~the~~ Figures 4a, 4b and 4c. It's observed that in the year 2000, the highest NDVI value was the maximum (0.824) in 2000. Whereas, the upper extreme value of NDVI gradually decreased in the subsequent study year and recorded as 0.626 in 2010 and 0.583 in 2020, which indicated the gradual depletion in the vegetation cover.

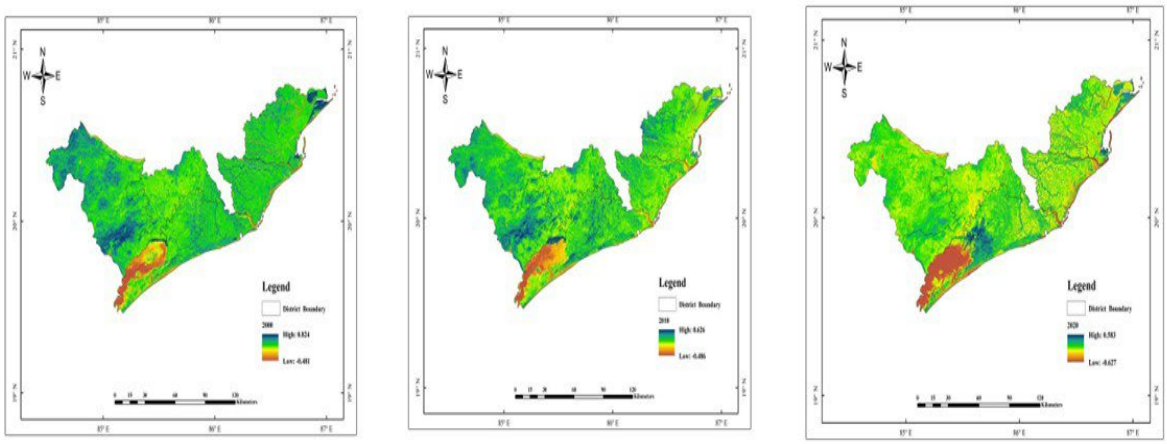

a. 2000 **b. 2010** **c. 2020**

Fig. 4(a-c) Spatial pattern of the NDVI of ESECPZ of Odisha over 2000-2020

The spatial pattern of NDBI during the study year was given in ~~the~~ Figures 5a, 5b and 5c. The temporal trend of NDBI was found to be just opposite to the trend of NDVI. The results inferred that the highest NDBI values gradually increased from 0.423 in 2000 to 0.638 in 2010 and 0.820 in 2020. This upward trend in NDBI values indicate~~d~~ a progressive expansion of the built-up area in the East and Southeastern Coastal Plain Zone of Odisha over the study period.

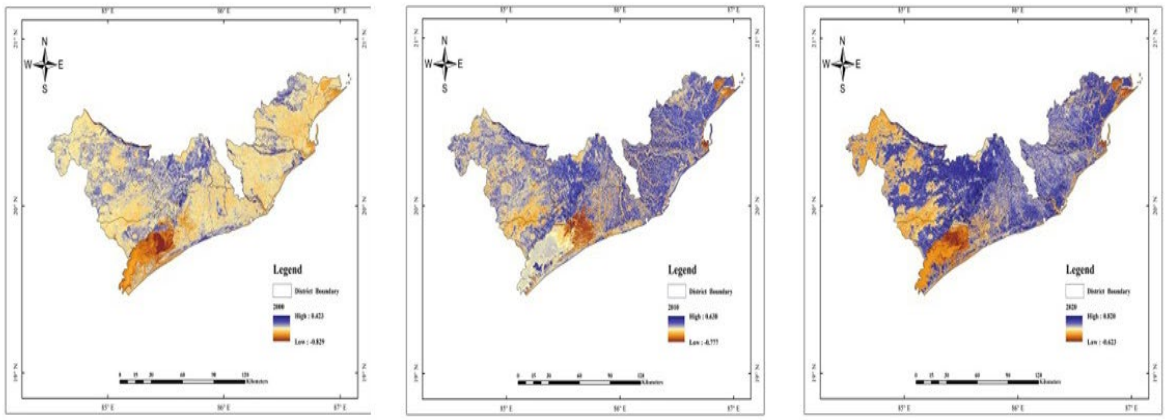

a. 2000 **b. 2010** **c. 2020**

Fig. 5(a-c) Spatial pattern of the NDBI of ESECPZ of Odisha over 2000-2020

3.4 Effect of Urbanization on LST

To ascertain the connection between LST and urbanization, a correlation study was carried out and the results have been given in ~~the~~ Table 8. The maximum LST exhibited a strong positive

correlation with the settlements, as indicated by the high value of correlation coefficient (0.95). Similarly, the positive agreement between minimum LST and settlements was noted with a correlation coefficient of 0.806. However, the correlation coefficient between the average LST and the settlements was determined as 0.955, indicating a strong positive correlation. Conversely, a strong inverse relationship was found between the surface vegetation cover and LST, as reflected by the negative relation between LST and NDVI in all the three years under consideration (Fig. 6). The values of the coefficient of determination (R^2) indicated that the variation in NDVI could explain the changes in LST by 68.2 % in 2000, 63.2 % in 2010 and 61.1 % in 2020. Whereas, a positive relationship was found between LST and NDBI. The results revealed that the NDBI explained maximum variation in LST by 72.2% in 2020, followed by 72.1% and 63 % in 2010 and 2000 respectively.

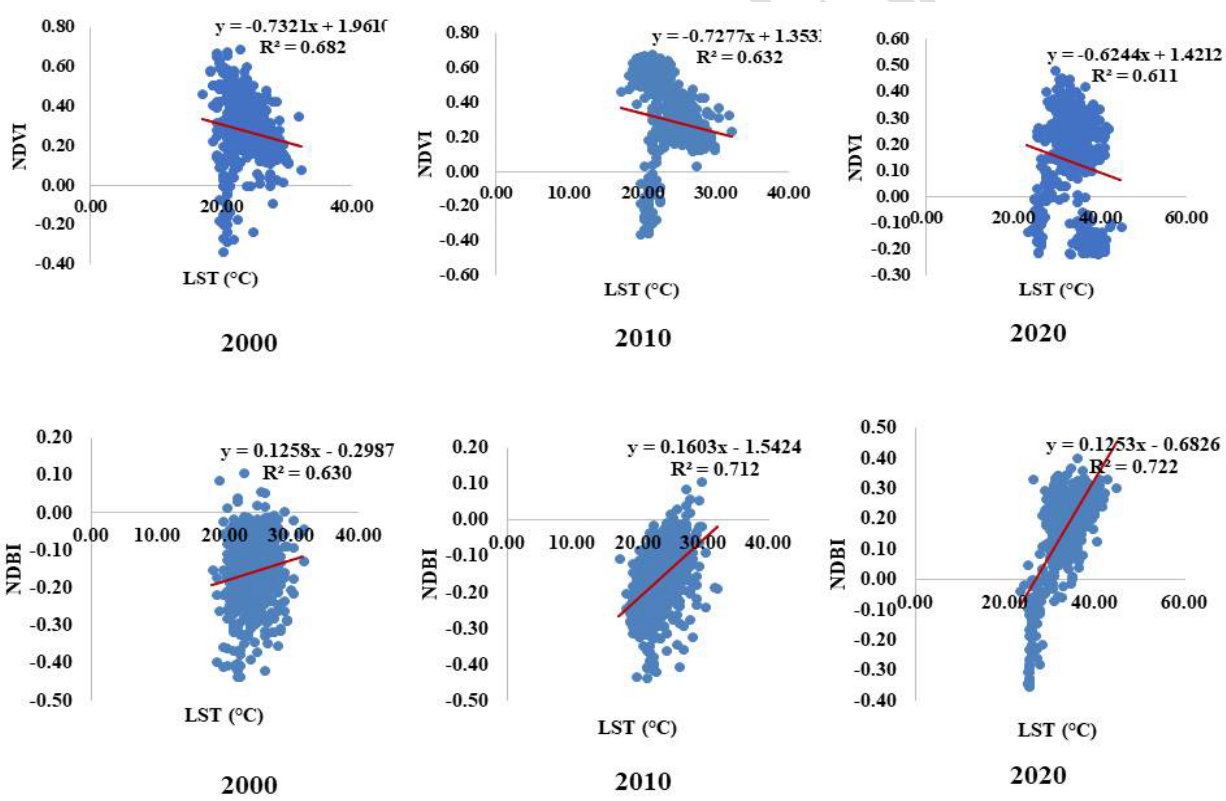

Fig. 6 Relationship of LST with NDVI and NDBI over the study period

4. Discussion

The present study applied the multi-temporal Landsat data, including Landsat 5 MSS, Landsat 7 ETM+ and Landsat 8 OLI & TRIS successfully for LULC change monitoring and estimating urbanization extent with higher accuracy. The legacy of the Landsat data maintaining the spatial and temporal resolution make it very much applicable for historical LULC change analysis (Dutrieux *et al*., 2016; Souza *et al*., 2020). Several earlier researches proved the applicability of multi-year Landsat data for monitoring urbanization with great accuracy (Dou and Chen, 2017). In the present study, the supervised classification resulted in very high accuracies with almost more than 80% overall accuracy and a kappa coefficient more than 0.80 which indicated a perfect agreement (0.81- 1.00) between predefined producer ratings and user assigned ratings (Meer & Mishra, 2020; Ghosh *et al*., 2022).

The current study provides~~d~~ convincing evidence that, during the course of the study period, some land cover types, such as forests and agricultural land, have been gradually disappearing. Conversely, the area set aside for settlements has been growing at a noticeably quicker pace. However, forests being an important land cover type in Odisha's East and Southeastern Coastal Plain Zone, observed gradual decrease over the past 20 years. This originally forested area has seen considerable portioning for urban development. The decline in forest areas due to developmental activities is in line with findings reported by Mishra *et al*. (2022). The findings infer~~red~~ that encroachments for a variety of objectives, such as road construction, mining, industrial growth, agricultural development, and other land development activities.

The capital of Odisha, Bhubaneswar, is situated in the East and Southeastern Coastal Plain Zone. Due to its tremendous population expansion, Bhubaneswar has seen quick development and construction (Tiwari, 2011; Swain *et al*., 2016; Swain *et al*., 2017). The majority of urbanization has come at the expense of reclaiming wetlands or converting agricultural land. Over the past 15 years, the land cover of Bhubaneswar has changed significantly, with a rise in urbanization of 83 percent. In a similar vein, during the course of these 15 years, from 2000 to 2014, there was a significant 89% decline in dense vegetation over the city and 83% decrease in agriculture fields. In the study area, rapid population increase accelerated the rate of urbanization. Puri (prominent destination for pilgrims) district in the study area, experienced rapid expansion due to rising urbanization. Puri's drawbacks include rising disparities between urban and rural areas and the migration of people from rural to urban areas in search of better economic opportunities. The town's decadal growth rate is 23.9%, which is continuing to grow both horizontally and vertically in the twenty-first century (Mishra *et al*., 2020). More than one-third of the East and

Southeastern Coastal Plain zone of Odisha is made up of agricultural land, which makes up the majority of the land cover in the study area. But from 2000 to 2020, the area of the agricultural land significantly decreased as a result of strong urbanization pressures, as noted by Gogoi *et al*. (2019).

The spatiotemporal change in LULC is identified to be one of the major factors responsible for changes in UHI effect over the city (Yan *et al*., 2016). Numerous previous studies have linked the anthropogenic changes in surface shape brought about by urbanization to notable adjustments in the local surface energy balance, which in turn creates a brand-new, local microclimate. There has been an increase in LST of about 5°C in the low temperature range and 3°C in the high temperature range, from 2000 to 2020. This rise in temperature can be attributed to increased urbanization. As noted by Liaquat *et al.* (2018), areas with more developed infrastructure tend to exhibit higher temperatures compared to their surroundings. The increase in land surface temperatures is largely due to the growth of populated regions. The metropolitan regions in the East and Southeastern Coastal Plain Zones of Odisha are experiencing a heat-island effect, which can also be attributed to this. In addition, other elements that may contribute to the increase in land surface temperatures include the spread of arid regions, deforestation, or a decrease in the amount of vegetation cover. Buildings, roads, industries, and other land-use purposes are examples of impermeable surfaces that can both absorb shortwave incoming solar radiation and help reduce outgoing longwave terrestrial emissions, both of which have a direct impact on the LST (Das *et al*., 2021). According to Fischer *et al*. (2012), under global warming, the surrounding rural areas would not experience nearly as much heat stress as the urban areas, and this difference in heat stress would become even more noticeable during heat waves. The ESECPZ's growing frequency of heat waves is evidence of the detrimental effects of urbanization and LULC change on the region's temperature (Gouda *et al*., 2017; Guleria and Gupta, 2019; Nageswararao *et al.,* 2020; Neethu *et al*., 2020; Boyaj *et al*., 2023).

Over the course of the investigation, a progressive decline in NDVI was seen. Lower NDVI values were seen in the middle region in 2000 and by 2020, these values had shifted to the western and eastern edges, indicating less vegetation or sparse flora. The study area's rising urbanization is the cause of the lowest NDVI values in 2020, which is in line with research showing that deterioration from the conversion of the original vegetated surface to the urbanized impervious surface resulted in lowering of NDVI (Du *et al*., 2019). According to Mathew *et al*. (2015), abundant urban regions are denoted by high NDBI values, whereas agrarian and aquatic

areas are indicated by low values. In ESECPZ, the eastern and western borders saw an expansion of higher NDBI values by 2020. It can be inferred from this that rising urbanization is the cause of the higher NDBI values in 2020.

LST, NDVI and NDBI are closely related (Marzban *et al*., 2018; Fatemi and Narangifard, 2019; Malik *et al*., 2019; Alademomi *et al*., 2022). Through image correlation analysis, it was determined that vegetated regions exhibit a negative correlation with LST, whereas built-up areas demonstrated a strong positive correlation with LST. By using image correlation analysis, it was discovered that built-up areas show a strong positive association with LST, while vegetative zones show a negative correlation (Molnar, 2016). The findings indicated that the study area had a notable rise in land surface temperature between 2010 and 2020, as a result of increasing urbanization. The greatest positive connection was observed between LST and NDBI, whereas the lowest negative correlation was observed between LST and NDVI in 2020.

5. Conclusion

The LULC of East and Southeastern Coastal Plain Zone of Odisha had undergone major changes from 2000 to 2020. The forest cover was rapidly diminishing, while settlements were experiencing substantial growth over a 20-year period. The study highlighted significant changes in three primary classes, viz., agriculture, forest land, and settlements. These changes have been driven by the imperative to accommodate the needs of a growing population, resulting in positive growth in settlements and a progressive decrease in both forest coverage and agricultural land. The expanding urban areas negatively impacted on the LST. Notably, this research has provided valuable insights into the often-overlooked impacts of urbanization on factors such as LST and vegetation cover. By shedding light on these hidden facts, the present study contributes to a better understanding of the complex relationship between urban development and environmental changes. These findings offer a positive perspective for the future and can inform and bolster forward-thinking initiatives and applications aimed at addressing these challenges.

Although, development is essential to sustain economic growth and there is a need to provide housing to the increasing population, priority needs to be given to mitigate the urban heat island effects and thus strive for achieving sustainability. More investment in green spaces, such as parks, green roofs, and urban forests, to mitigate the urban heat island effect and reduce flooding is required. Encourage the construction of energy-efficient and climate-resilient buildings that can withstand extreme weather events. By implementing these recommendations,

urbanized areas can become more resilient to the impacts of climate change and create healthier, more sustainable communities for current and future generations.

Further, satellite imagery has improved significantly, but it is not always be sufficient to capture detailed urban features. This can make it challenging to monitor small-scale urban changes accurately. Tall buildings and vegetation can cast shadows or obscure other features, making it difficult to accurately identify and classify urban land cover. Despite these limitations, satellite remote sensing remains one of the most effective tools for monitoring urbanization at regional and global scales. Integrating satellite data with other sources of information, such as aerial imagery, ground surveys, and census data, can help overcome some of these limitations and provide a more comprehensive understanding of urbanization processes.

Data availability statement

Data will be made available on reasonable request.

Declaration of competing interest

The authors declare no conflicts of interest/competing interests.

References

Alademomi, A. S., Okolie, C. J., Daramola, O. E., Akinnusi, S. A., Adediran, E., Olanrewaju, H. O., ... & Odumosu, J. (2022). The interrelationship between LST, NDVI, NDBI, and land cover change in a section of Lagos metropolis, Nigeria. *Applied Geomatics*, *14*(2), 299-314.

Argüeso, D., Evans, J. P., Fita, L., & Bormann, K. J. (2014). Temperature response to future urbanization and climate change. Climate dynamics, 42, 2183-2199.

Bai, X., McPhearson, T., Cleugh, H., Nagendra, H., Tong, X., Zhu, T., & Zhu, Y. G. (2017). Linking urbanization and the environment: Conceptual and empirical advances. Annual review of environment and resources, 42, 215-240.

Bonafoni, S., & Keeratikasikorn, C. (2018). Land surface temperature and urban density: Multiyear modeling and relationship analysis using MODIS and Landsat data. Remote Sensing, 10(9), 1471.

Bouhennache, R., Bouden, T., Taleb-Ahmed, A., & Cheddad, A. (2019). A new spectral index for the extraction of built-up land features from Landsat 8 satellite imagery. Geocarto International, 34(14), 1531-1551.

Boyaj, A., Nadimpalli, R., Reddy, D., Sinha, P., Karrevula, N. R., Osuri, K. K., ... & Kaginalkar, A. (2023). Role of radiation and canopy model in predicting heat waves using WRF over the city of Bhubaneswar, Odisha. *Meteorology and Atmospheric Physics*, *135*(6), 60.

Chakrabarti, P. D. (2001). Urban crisis in India: new initiatives for sustainable cities. *Development in practice*, *11*(2-3), 260-272.

Chapman, S., Watson, J. E., Salazar, A., Thatcher, M., & McAlpine, C. A. (2017). The impact of urbanization and climate change on urban temperatures: a systematic review. Landscape Ecology, 32, 1921-1935.

Chen, F., Yang, X., & Zhu, W. (2014). WRF simulations of urban heat island under hot-weather synoptic conditions: The case study of Hangzhou City, China. Atmospheric research, 138, 364-377.

Chen, Y. C., Chiu, H. W., Su, Y. F., Wu, Y. C., & Cheng, K. S. (2017). Does urbanization increase diurnal land surface temperature variation? Evidence and implications. Landscape and Urban Planning, 157, 247-258.

Das, N., Mondal, P., Sutradhar, S., & Ghosh, R. (2021). Assessment of variation of land use/land cover and its impact on land surface temperature of Asansol subdivision. *The Egyptian Journal of Remote Sensing and Space Science*, *24*(1), 131-149.

Dou, P., & Chen, Y. (2017). Dynamic monitoring of land-use/land-cover change and urban expansion in Shenzhen using Landsat imagery from 1988 to 2015. *International Journal of Remote Sensing*, *38*(19), 5388-5407.

Du, J., Fu, Q., Fang, S., Wu, J., He, P., & Quan, Z. (2019). Effects of rapid urbanization on vegetation cover in the metropolises of China over the last four decades. *Ecological Indicators*, *107*, 105458.

Dutrieux, L. P., Jakovac, C. C., Latifah, S. H., & Kooistra, L. (2016). Reconstructing land use history from Landsat time-series: Case study of a swidden agriculture system in Brazil. *International Journal of Applied Earth Observation and Geoinformation*, *47*, 112-124.

Falkner, R. (2016). The Paris Agreement and the new logic of international climate politics. *International Affairs*, *92*(5), 1107-1125.

Fatemi, M., & Narangifard, M. (2019). Monitoring LULC changes and its impact on the LST and NDVI in District 1 of Shiraz City. *Arabian Journal of Geosciences*, *12*(4), 127.

Fischer, E. M., Oleson, K. W., & Lawrence, D. M. (2012). Contrasting urban and rural heat stress responses to climate change. Geophysical research letters, 39(3).

Gogoi, P. P., Vinoj, V., Swain, D., Roberts, G., Dash, J., & Tripathy, S. (2019). Land use and land cover change effect on surface temperature over Eastern India. Scientific reports, 9(1), 8859.

Gouda, K. C., Sahoo, S. K., Samantray, P., & Himesh, S. (2017). Simulation of extreme temperature over Odisha during May 2015. *Weather and Climate Extremes*, *17*, 17-28.

Guleria, S., & Gupta, A. K. (2018). Heat wave in India documentation of state of Telangana and Odisha (2016). *National Institute of Disaster Management, New Delhi*, 124.

Güneralp, B., Reba, M., Hales, B. U., Wentz, E. A., & Seto, K. C. (2020). Trends in urban land expansion, density, and land transitions from 1970 to 2010: A global synthesis. Environmental Research Letters, 15(4), 044015.

Halder, B., & Bandyopadhyay, J. (2021). Evaluating the impact of climate change on urban environment using geospatial technologies in the planning area of Bilaspur, India. *Environmental Challenges*, *5*, 100286.

Irfeey, A. M. M., Chau, H. W., Sumaiya, M. M. F., Wai, C. Y., Muttil, N., & Jamei, E. (2023). Sustainable mitigation strategies for urban heat island effects in urban areas. *Sustainability*, *15*(14), 10767.

Karanam, H. K., & Neela, V. B. (2017). Study of normalized difference built-up (NDBI) index in automatically mapping urban areas from Landsat TN imagery. Int J Eng Sci Math, 8, 239-48.

Kumari, B., Tayyab, M., Shahfahad, Salman, Mallick, J., Khan, M. F., & Rahman, A. (2018). Satellite-driven land surface temperature (LST) using Landsat 5, 7 (TM/ETM+ SLC) and Landsat 8 (OLI/TIRS) data and its association with built-up and green cover over urban Delhi, India. Remote Sensing in Earth Systems Sciences, 1, 63-78.

Liaqut, A., Younes, I., Sadaf, R., & Zafar, H. (2019). Impact of urbanization growth on land surface temperature using remote sensing and GIS: a case study of Gujranwala City, Punjab, Pakistan. *International Journal of Economic and Environmental Geology*, 44-49.

Lohani, T. K. (2022). Causes, Effects, and Remedial Measures of Climate Change in the East Coast of India with Special Reference to the State of Odisha. In India II: Climate Change Impacts, Mitigation and Adaptation in Developing Countries (pp. 383-406). Cham: Springer International Publishing.

Macintyre, H. L., Heaviside, C., Taylor, J., Picetti, R., Symonds, P., Cai, X. M., & Vardoulakis, S. (2018). Assessing urban population vulnerability and environmental risks across an urban area during heatwaves–Implications for health protection. Science of the total environment, 610, 678-690.

Malik, M. S., Shukla, J. P., & Mishra, S. (2019). Relationship of LST, NDBI and NDVI using landsat-8 data in Kandaihimmat watershed, Hoshangabad, India. Indian Journal of Geo Marine Sciences, 48(1): 25- 31

Marzban, F., Sodoudi, S., & Preusker, R. (2018). The influence of land-cover type on the relationship between NDVI–LST and LST-T air. *International Journal of Remote Sensing*, *39*(5), 1377-1398.

Meer, M. S., & Mishra, A. K. (2020). Remote sensing application for exploring changes in land-use and land-cover over a district in Northern India. Journal of the Indian Society of Remote Sensing, 48, 525-534.

Mishra, M., Santos, C. A. G., do Nascimento, T. V. M., Dash, M. K., da Silva, R. M., Kar, D., & Acharyya, T. (2022). Mining impacts on forest cover change in a tropical forest using remote sensing and spatial information from 2001–2019: A case study of Odisha (India). *Journal of Environmental Management*, *302*, 114067.

Mishra, S. P., Sethi, K. C., Swain, N. M.., Behera, S. S., Siddique, M. (2020). Anthropocene Water-Body Changes in Coastal Towns, Puri, Odisha: Micro-Scale Geospatial Analysis. Indian Journal of Natural Sciences, 10 (59): 18190- 18200

Mohajerani, A., Bakaric, J., & Jeffrey-Bailey, T. (2017). The urban heat island effect, its causes, and mitigation, with reference to the thermal properties of asphalt concrete. Journal of environmental management, 197, 522-538.

Molnár, G. (2016). Analysis of land surface temperature and NDVI distribution for Budapest using Landsat 7 ETM+ data. *Acta climatologica et chorologica*, *49*, 49-61.

Motesharrei, S., Rivas, J., Kalnay, E., Asrar, G. R., Busalacchi, A. J., Cahalan, R. F., ... & Zeng, N. (2016). Modeling sustainability: population, inequality, consumption, and bidirectional coupling of the Earth and Human Systems. National Science Review, 3(4), 470-494.

Nagendra, H., Bai, X., Brondizio, E. S., & Lwasa, S. (2018). The urban south and the predicament of global sustainability. Nature sustainability, 1(7), 341-349.

Nageswararao, M. M., Sinha, P., Mohanty, U. C., & Mishra, S. (2020). Occurrence of more heat waves over the central east coast of India in the recent warming era. *Pure and Applied Geophysics*, *177*, 1143-1155.

Nayak, S. K., & Nandimandalam, J. R. (2023). Impacts of climate change and coastal salinization on the environmental risk of heavy metal contamination along the odisha coast, India. Environmental Research, 238, 117175.

Neethu, C., Ramesh, K. V., & Shafeer, K. B. (2020). Understanding the spatio-temporal structure of recent heat waves over India. *Natural Hazards*, *102*(2), 673-688.

Parapurath, F., Rath, B. S., & Manikandan, N. (2020). Forest cover classification and change detection using NDVI over 1990 to 2020 in the Western Central Table Land Zone of Odisha. *Forest*, *745*(2592.5), 3970-91.

Parapurath, F., Waquar, T., Lalmuanzuala, B., & Prakash, A. (2025a). GLOBAL WARMING SOLUTIONS: HARNESSING AI, ML & ADVANCED TECHNOLOGIES FOR A SUSTAINABLE FUTURE. *AgriGate-An International Multidisciplinary e-Magazine, 5*(9), 826-840.

Parapurath, F., Senapati, R., Ghosh, A., Rath, B. S., & Verma, D. (2025b). Spatio-temporal changes of the forest cover in North Eastern Ghat Zone of Odisha, India, using multi-year Landsat data. *Nature Environment and Pollution Technology*, *24*(3), B4291.

Peng, J., Ma, J., Liu, Q., Liu, Y., Li, Y., & Yue, Y. (2018). Spatial-temporal change of land surface temperature across 285 cities in China: An urban-rural contrast perspective. Science of the Total Environment, 635, 487-497.

Prakash, A., Parapurath, F., Nazar, S., Meena, A. K., Panchulakshmi, M., & Waquar, T. (2025). APPLICATION OF GIS TECHNOLOGY FOR RESTORATION OF GROUNDWATER RESOURCES: A COMPREHENSIVE REVIEW. *Plant Archives*, *25*(2), 2127-2136.

Roy, P. S., Ramachandran, R. M., Paul, O., Thakur, P. K., Ravan, S., Behera, M. D., ... & Kanawade, V. P. (2022). Anthropogenic land use and land cover changes—A review on its environmental consequences and climate change. *Journal of the Indian Society of Remote Sensing*, *50*(8), 1615-1640.

Senapati, R., Rath, B. S., Parapurath, F., Mahanty, M., Ghosh, A., Meena, A. K., & Pandit, R. (2024). Forest Cover Change Detection Over North Eastern Ghat Zone of Odisha, India Using Multi-Year Landsat Data. *International Journal of Environment and Climate Change*, *14*(9), 787-795.

Sidiqui, P., Huete, A., & Devadas, R. (2016). Spatio-temporal mapping and monitoring of Urban Heat Island patterns over Sydney, Australia using MODIS and Landsat-8. In 2016 4th International Workshop on Earth observation and Remote Sensing applications (EORSA) (pp. 217-221). IEEE.

Souza Jr, C. M., Z. Shimbo, J., Rosa, M. R., Parente, L. L., A. Alencar, A., Rudorff, B. F., ... & Azevedo, T. (2020). Reconstructing three decades of land use and land cover changes in brazilian biomes with landsat archive and earth engine. *Remote Sensing*, *12*(17), 2735.

Subba Rao, A. V. M., Parapurath, F., Sarath Chandran, M. A., Bal, S. K., Manikandan, N., & Singh, V. K. (2025). Spatiotemporal variability and trends of hailstorms over India. *Natural Hazards*, *121*(2), 1687-1710.

Tam, B. Y., Gough, W. A., & Mohsin, T. (2015). The impact of urbanization and the urban heat island effect on day to day temperature variation. Urban Climate, 12, 1-10.

Van Vuuren, D. P., Stehfest, E., Gernaat, D. E., Doelman, J. C., Van den Berg, M., Harmsen, M., ... & Tabeau, A. (2017). Energy, land-use and greenhouse gas emissions trajectories under a green growth paradigm. Global environmental change, 42, 237-250.

Virtudes, A., Abbara, A., & Sá, J. (2017). Dubai: A pioneer smart city in the Arabian territory. In IOP Conference Series: Materials Science and Engineering (Vol. 245, No. 5, p. 052071). IOP Publishing.

Wang, J., Feng, J., & Yan, Z. (2015). Potential sensitivity of warm season precipitation to urbanization extents: Modeling study in Beijing-Tianjin-Hebei urban agglomeration in China. Journal of Geophysical Research: Atmospheres, 120(18), 9408-9425.

Wei, Y., Chen, H., & Huang, J. J. (2024). Response of surface energy components to urban heatwaves and its impact on human comfort in coastal city. Urban Climate, 54, 101836.

Wu, C., Li, J., Wang, C., Song, C., Chen, Y., Finka, M., & La Rosa, D. (2019). Understanding the relationship between urban blue infrastructure and land surface temperature. Science of the Total Environment, 694, 133742.

Yan, Z. W., Wang, J., Xia, J. J., & Feng, J. M. (2016). Review of recent studies of the climatic effects of urbanization in China. Advances in Climate Change Research, 7(3), 154-168.

Zhao, N., Jiao, Y., Ma, T., Zhao, M., Fan, Z., Yin, X., ... & Yue, T. (2019). Estimating the effect of urbanization on extreme climate events in the Beijing-Tianjin-Hebei region, China. Science of the total environment, 688, 1005-1015.